TRANSACTIONS OF THE INSTITUTE OF FLUID-FLOW MACHINERY

No. 127, 2015, 117–136

WIESŁAW OSTACHOWICZ,[1] TOMASZ WANDOWSKI, PAWEŁ MALINOWSKI

Principles of piezo-based machinery health monitoring

The Szewalski Institute of Fluid-Flow Machinery of the Polish Academy of Sciences, Mechanics of Intelligent Structures Department, Fiszera 14, 80-231 Gdańsk, Poland

Abstract

In this paper methods used for structural health monitoring of machinery parts are discussed. These methods are based on applications of piezoelectric transducers. Proposed methods are used for assessment of structural machine parts manufactured of carbon fiber reinforced plastics/polymers (CFRP) and glass fiber reinforced plastics/polymers (GFRP). The first discussed method is based on elastic wave propagation and scanning laser vibrometry. This method is based on the fact that any kind of structural discontinuities cause changes in elastic wave propagation within the structure. In the proposed approach elastic waves are generated using piezoelectric transducer and then the waves are registered using scanning laser vibrometer. Here attention was paid on an analysis of elastic wave propagation in simple composite parts and parts with complex structure. The paper presents also results of simulated damage localization. The second method is an electromechanical impedance (EMI) technique. In this case piezoelectric transducer is also effectively used. This transducer is attached to an investigated structure. Due to electromechanical coupling of piezoelectric transducer and a structure, characteristics of mechanical resonances of the structure can be registered through the measurement of electrical parameters of piezoelectric transducer. An initiation of damage causes changes in resonant characteristics of considered structures. As electrical parameter very often impedance, admittance, resistance, conductance or reactance are used. For that purpose electrical impedance analyzer is used. Three parameters have been taken for the analysis. For proposed method effective damage indexes have been proposed.

[1]Corresponding author. E-mail address: wieslaw@imp.gda.pl

Keywords: Laser vibrometry; LDV; Electromechanical impedance; EMI damage localization; Composites;

1 Introduction

Structural health monitoring (SHM) is a methodology aiming at assessment of the state of structures in real time. One of the promising SHM techniques is based on piezoelectric sensors (PZT). The PZT are very light, thin and can be used as actuators and sensors due to piezoelectric effect. Piezoelectric sensors can be used to generate and receive elastic waves [1]. Elastic wave propagation method can be used for damage localization in very simple structural elements like rods [2,3], beams [4], and pipes [5,6]. However large number of papers are related to topic of damage detection and localization in metallic as well as composite plates [1,7,8]. Also in more complicated structures elastic wave propagation method was used in order to localize damage. In the work [9] damage localization was performed in aluminum panel with honeycomb core. Damage detection was also conducted in the case of bolted steel members [10] and riveted spacecraft-like panels [11]. Generally two approaches of elastic wave propagation method are used, taking into account method of actuation and sensing: pitch–catch [12,13] and pulse–echo [4,12]. In the pulse echo approach also phased array technique [1,5,9] can be recognized. It should be also mentioned that Giurgiutiu and Soutis introduced third approach called thickness mode [14]. These same authors also specified fourth approach called impact/AE detection. This method is used for impact source location and it is a passive method contrary to the three above mentioned active methods. Elastic wave–based methods allow to detect such damage like: fatigue crack [15,16], corrosion [7,11], delamination/debonding [2,4,17], impact caused damage, for example crushing over multiple honeycomb cells [9], or broken fibers [12]. Recently many researchers are interested in investigation of moisture absorption influence, particularly on Lamb wave propagation in viscoelastic carbon fiber reinforced plastics/polymer (CFRP) [18]. SHM systems can be used in many fields like aerospace structures [11,12], civil engineering structures (e.g., bridges), [19], and offshore engineering (i.e., wind turbines).

The second piezo-based method is the electromechanical impedance (EMI). It can be treated as supporting for elastic wave–based method because it diagnoses the sensor itself and also the surrounding area. During the measurements basic electric parameters of the sensor are gathered. Parameters

such as resistance, reactance, impedance, conductance, etc., are measured and analyzed. Appearance of additional resonance peaks, peak shift in frequency or magnitude change can be treated as indicator of defect of the host structure [20]. The EMI technique has been successful used to diagnose the piezoelectric transducer, embedded in composite material [21,22]. The EMI technique was a basis for crack detection in thin plates, i.e., in the research reported in [23]. In the work [24] damage localization method was developed using EMI and application of artificial neural networks (ANN). Electromechanical impedance has been used for assessment of beams [25], plates [1,26], railroad tracks [27], pipes with bolted joints [25], bonded joints [28], concrete structures [29], and riveted panels [30,31].

In this paper the authors focus on the previously mentioned two methods. In their investigations the elastic wave based method has been combined with laser Doppler vibrometer (LDV) for noncontact sensing of the propagating waves. Both LDV and EMI methods has been used for SHM of composite structural elements.

The paper is structured as follows. In the second section LDV technique is described. In the third Section the results for LDV method are provided. In the fourth Section EMI method is presented and it is followed by EMI results in subsequent section. The last Section concludes the conducted research.

2 LDV technique for guided elastic waves sensing

Laser Doppler vibrometry (LDV) is a noncontact measurement technique that allows to register velocities or displacements of structural vibrations. This technique can be successfully used for measurements of standing waves as well as guided waves propagating in the structure. This technique is also named SLDV when scanning laser Doppler vibrometer is used. In experimental research authors used Polytec 3D scanning laser Doppler vibrometer PSV400. The vibrometer is able to measure 3D components of vibration velocities (out-of-plane and in-plane components). However during the research all measurements were performed in 1D scanning mode which allow to measure only out-of-plane vibration velocity component. The registered signals were related to guided waves propagating in the composite structural components. Guided waves were excited using internal signal generator installed in PSV400 vibrometer. The signal has been sent from generator to SONOX P5 transducer, in the form of disc with diameter 10 mm and thick-

ness 0.5 mm. Scanning measurements performed for surface of investigated structure allowed to visualize guided wave propagation. This measurement approach is named full wavefield approach.

3 Results for LDV

In the Fig. 1 results for such measurements are presented in the form of arbitrary chosen frames taken from animation of guided wave propagation. These measurements were performed for panel manufactured of glass fibre reinforced plastic/polymer (GFRP). The dimensions of the panel were equal 400 mm × 400 mm × 1.5 mm. Damage was simulated as 25 mm long notch, and 0.5 mm deep. Guided waves were excited by the piezoelectric transducer located in the middle of the panel. The excitation signal was assumed in the form of tone burst signal with five cycles and carrier frequency 100 kHz. In Fig. 1a it can be easily noticed that two guided wave modes propagate in the panel. Two modes can be clearly recognized as their wave lengths differs. Moreover this mode with larger wavelength propagate with higher velocity and it is approximation of fundamental symmetric Lamb wave mode noted as S_0. It can be noticed that its velocity of propagation strongly depends on the direction of propagation. The velocity is much higher in the horizontal direction than in vertical direction – the wavefront shape is elliptical. This is caused by internal structure of composite panel and strictly depend on orientation of internal layers with glass fibre reinforcement. In this case all layers are oriented horizontally $[0, 0, 0, 0, 0]^{\circ}$.

The second propagating mode has smaller wave length and propagates much slower. This is approximation of fundamental antisymmetric Lamb wave mode noted as A_0. It can be noticed that for this mode differences in velocities for horizontal and vertical direction are smaller, however elliptical shape of propagating wave front can be easily noticed in Fig. 1b. In this figure also a wave reflection related to this mode and caused by introduced notch can be noticed. It should be emphasized that there was no interaction of wave mode S_0 with notch due to too large wave length of this mode in relation to notch size.

In the Fig. 2 the frames taken out from animation of guided wave propagation in GFRP panel with dimensions: 440 mm × 440 mm × 1.5 mm are presented. In the considered example damage was simulated by introduced delamination which was created using heat gun. The orientation of glass fiber layers has been the same as in previous example. The frequency of ex-

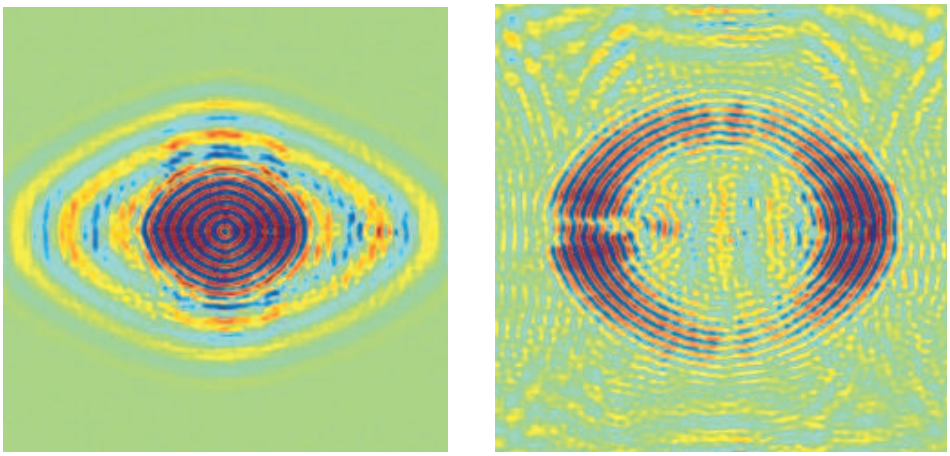

a) b)

Figure 1: Chosen frames from animation of elastic guided wave propagation in GFRP panel with notch: a), b) chosen time frames for excitation frequency 100 kHz.

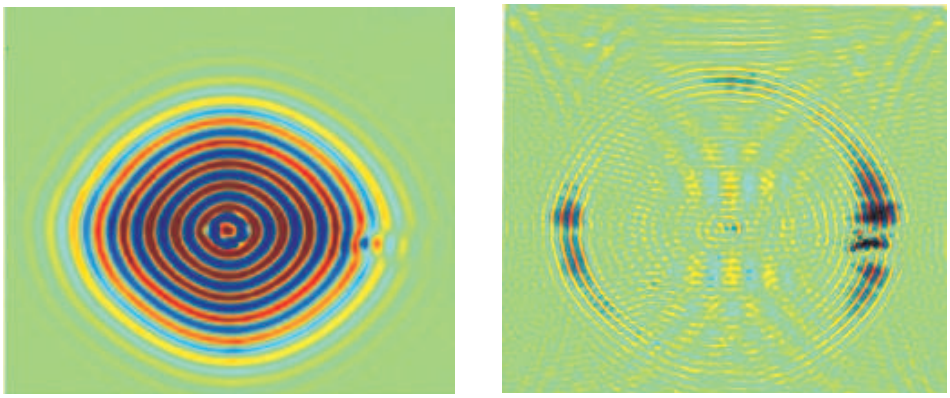

a) b)

Figure 2: Frames from animation of wave propagation in GFRP panel with delamination, excitation frequency: a) 16 kHz, b) 100 kHz.

citation was assumed as 16 kHz (Fig. 2a) and 100 kHz (Fig. 2b). Analyzing these results it can be noticed that there are wave interactions with delamination in both cases. These interactions can be noticed on the right hand side. Here the velocity of propagating wave mode also strongly depends on direction of propagation due to orthotropic properties of panel material.

Next step has been related to application of a damage detection algo-

rithm. For that purpose full-field measurements of guided wave propagation were conducted for GFRP panel with dimensions 400 mm × 400 mm × 1.5 mm. In the considered case the layer orientation was assumed in the form of [0, 90, 0, 90, 0]°.

The excitation signal was assumed in the form of five cycle tone burst with the carrier frequency 16 kHz. Elastic waves were generated by piezoelectric transducer located in the middle of the panel. Damage was simulated by an additional mass attached to the panel surface that is opposite to the scanned one. This mass was predicted in the form of steel disc with diameter 8 mm and 1 mm thickness. Two scenarios of additional mass location were investigated. Results in the form of two frames selected from the animation of elastic wave in GFRP panel with first simulated damage scenario are presented in Fig. 3. The elastic wave interation with additional mass is clearly visible in the upper part of frames illustrating wave propagation. Wave reflection from additional mass is clearly visible for the second frame.

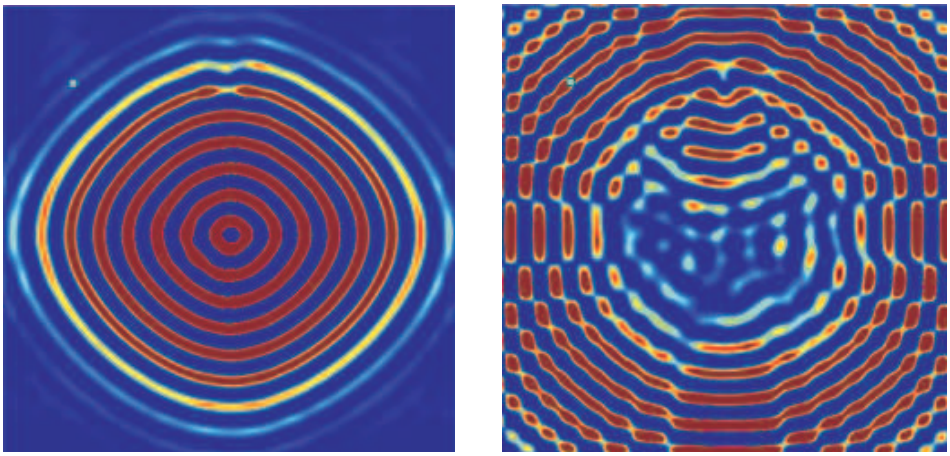

Figure 3: Frames from animation of elastic wave propagation in GFRP panel – first damage scenario.

Results for second simulated damage scenario are presented in Fig. 4. In the considered case the disturbance of elastic wave propagation caused by additional mass can be also clearly noticed.

Analysing frames illustrating wave propagation for both cases of damage scenario it can be noticed that in this case velocities of wave propagation in vertical and horizontal direction have similar values. This is due to glass

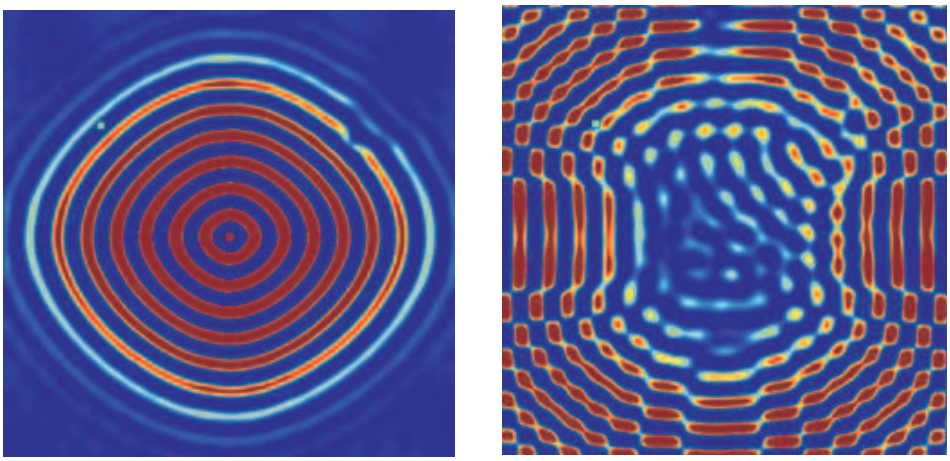

Figure 4: Frames from animation of elastic wave propagation in GFRP panel – second damage scenario.

fibre reinforcement orientation [0, 90, 0, 90, 0]°.

In order to brake damage localisation, algorithm that process full–field measurements of propagating wave was proposed. In this approach elastic wave signals need to be registered in the dense mesh of points created on the surface of structure in contrary to the point-wise approach, where wave propagation signals are register in small number of points. This registration is performed in real condition by using piezoelectric transducer.

In the case of full-field measurements very good results of structural discontinuity visualization can be achieved. This is caused due to large amount of received signals and data used for the process. Proposed damage localization algorithm maps registered signals into the surface of the structure by calculating the signal energy using the root mean square (RMS) index [31]. The RMS index for measurement point j was calculated from signal S of length N using the following formula:

$$RI_j = \sqrt{\frac{1}{N}\sum_{k=1}^{N} S_{j,k}^2}\,, \tag{1}$$

where subscript k denotes the time sample number. The proposed algorithm was tested for signals collected for two simulated damage scenarios. As results RMS energy maps were created for both cases (Figs. 5 and 6). Such a RMS map illustrates elastic wave energy distribution in the investigated GFRP panel. Analysing results presented in Figs. 5 and 6 it can

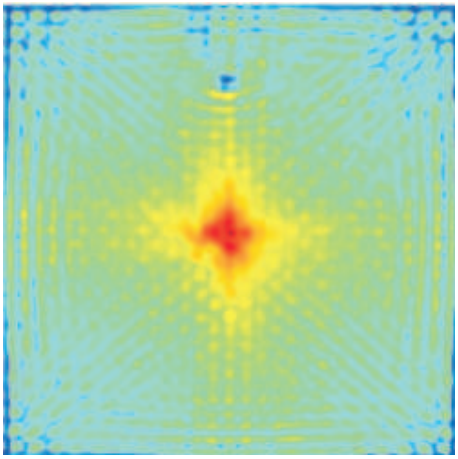

Figure 5: RMS energy map for additional mass – first scenario.

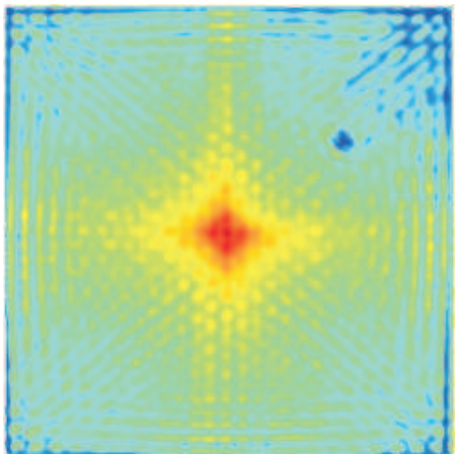

Figure 6: RMS energy map for additional mass – second scenario.

be noticed that in both damage scenarios changes in the wave energy distribution around damaged region can be clearly noticed. The region in the middle of a panel with higher energy is related to excitation of waves in this location.

Next step was related to the analysis of elastic wave propagation in composite panel of real engineering structure. In this research a fragment of a helicopter main rotor blade was used. This blade had a complex internal structure which consists of GFRP skin, GFRP I–section, honeycomb core and stiffeners (Fig. 7). The considered blade before measurements was covered by retro–reflective tape in order to enhance reflected laser signal of vibrometer. The wave signals were collected for two excitation frequencies 16 kHz and 50 kHz. Based on these signals RMS energy maps were created (Fig. 8). Analysing results for excitation frequency 16 kHz it can be seen that details of internal structure of the composite blade are accurately visualized. Due to elastic wave interaction with honeycomb core its cells can be clearly recognized. Elastic wave has been generated near the lower edge of blade on the left hand side. This place can be clearly visible on RMS maps because there is a maximum amplitude of the energy distribution. In the considered area composite profile is located that creating leading edge of the blade. The main part of wave energy is distributed in the leading edge profile. Its means that waves propagate mainly along this part. The smaller part of energy distribution is related to the propagation outside

Figure 7: Visible internal structure of helicopter main rotor blade.

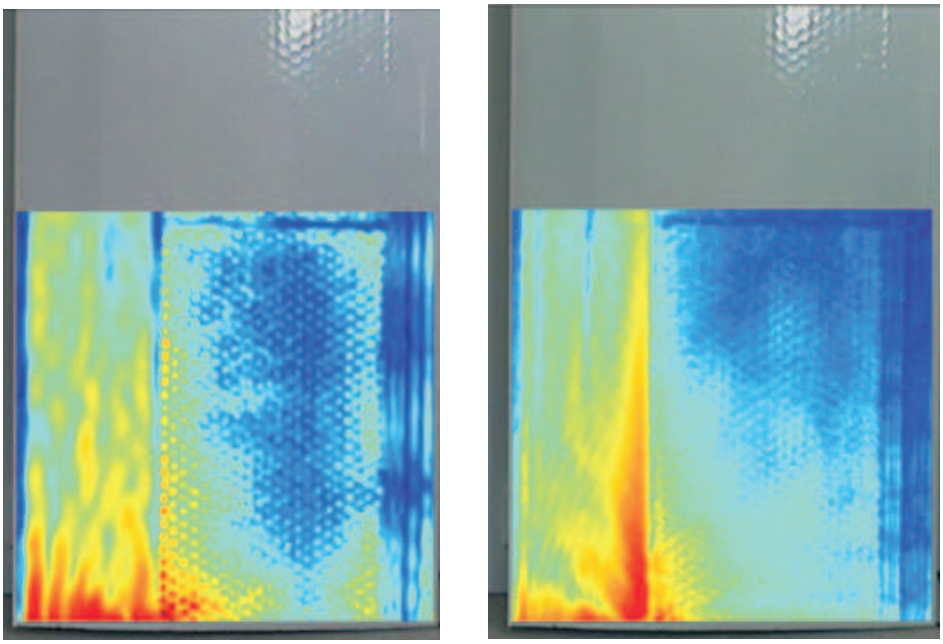

a) b)

Figure 8: RMS energy maps created for part of helicopter main rotor blade for excitation frequency: a) 16 kHz, b) 50 kHz.

this element. The elastic waves propagate in this case into the area where honeycomb core is located. On the right hand side trailing edge profile is

located with stiffeners that are visible as the region with very small contrast (low energy of the waves). In the top edge of the RMS maps at the end of honeycomb fulfilment also stiffener is clearly visible. In the case of excitation frequency equal to 50 kHz internal blade structure can be also noticed however in this case wave damping is much higher.

The last part of research related to this element was connected with damage detection. In this case guided wave measurements have been taken for referential and damaged state of the blade.

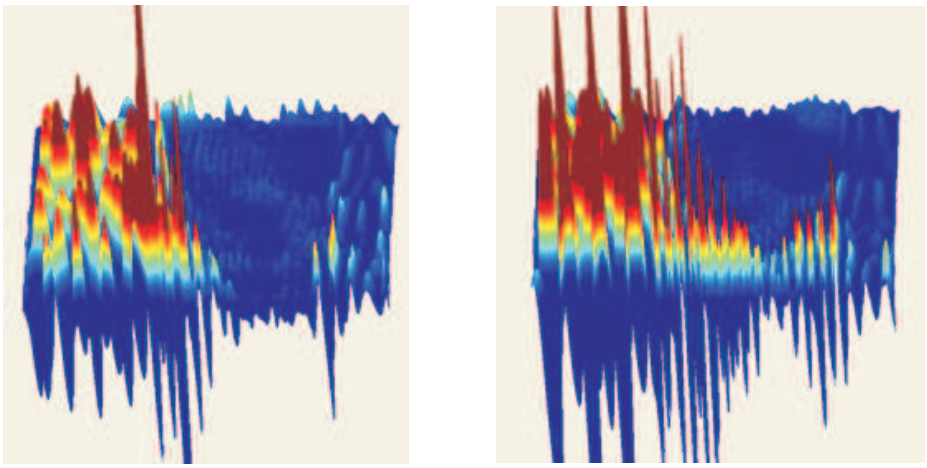

a) b)

Figure 9: Frames from animation of elastic wave propagation in blade in: a) referential state, b) damaged state (delamination)

An introduced damage was assumed in the form of delamination (separation of blade skin from honeycomb core) near the bottom blade edge. In Fig. 9 two frames from animation of elastic wave propagation in the blade with referential and damaged state are presented. These frames present wave propagation at the same time. Observing in Fig. 9a elastic wave propagation along the bottom edge (on the right) it can be noticed that waves are strongly damped by the honeycomb core. At the end of this section (connection of honeycomb and profile of trailing edge) strong wave reflection is noticed (Fig. 9a). Comparing these result with frame created for damaged state (Fig. 9b) it can be easily noticed that elastic waves are not as much damped in honeycomb core as in the referential state. This is caused by delamination due to which composite skin of blade is separated from honeycomb. The elastic waves propagate mainly in the skin which reduces the

damping. As the effect of this delamination, the amplitude in the end of the section (on the right) has larger amplitude than for the case of referential state. Due to generally large wavelength, the waves reflection from the delamination cannot be easily recognized.

4 EMI technique

The electromechanical impedance (EMI) method is considered as one of the NDT (non-destructive testing) or SHM (structural health monitoring) methods. It uses a piezoelectric sensor that is bonded to the inspected host structure. During the measurements, basic electric parameters of the sensor are gathered. Parameters such as resistance, reactance, impedance, conductance, etc., are measured and analyzed. These quantities are measured as a function of frequency. Due to direct and converse piezoelectric effect the sensor excites and senses the response from the host structure. This electromechanical coupling causes that the registered impedance spectra are modified by the presence of the host structure. If there is a damage or some other discontinuity it has also influence on the registered spectra. Appearance of additional resonance peaks, peak shift in frequency or magnitude change can be treated as indicator of defect of the host structure [20]. One also should not forget that the sensors for EMI technique is bonded to the structure and the bonding itself has an influence on the response [32–34].

In order to extract damage related features of the EMI spectra, various frequency bands are analyzed. These bands depend on the inspected structure and the used piezoelectric sensor. Some researchers limit themselves to the 100 kHz band, because they use AD5933 chip with limited frequency range [35]. The authors of work [36] underline the good sensitivity of the EMI method based on an analysis of the thickness vibration mode of the considered piezoelectric sensors.

5 EMI results

In the investigations a CFRP sample has been considered that was cut out from a larger panel. The panel was manufactured of prepregs and it was taken from AW139 helicopter fuselage. The investigated sample had the following dimensions: 250 mm × 200 mm, and it is depicted in Fig. 10. The damage was simulated by a surface cut with two lengths, 5 and 10 mm. It has been located 50 mm to the left from the sample center.

The electromechanical impedance was measured by a piezoelectric sensor installed at the middle of the sample surface.

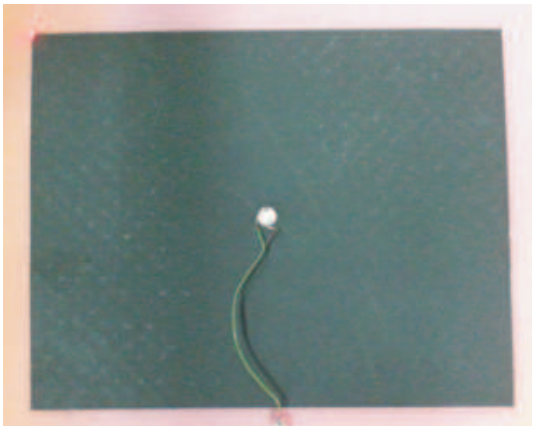

Figure 10: CFRP sample investigated with EMI method.

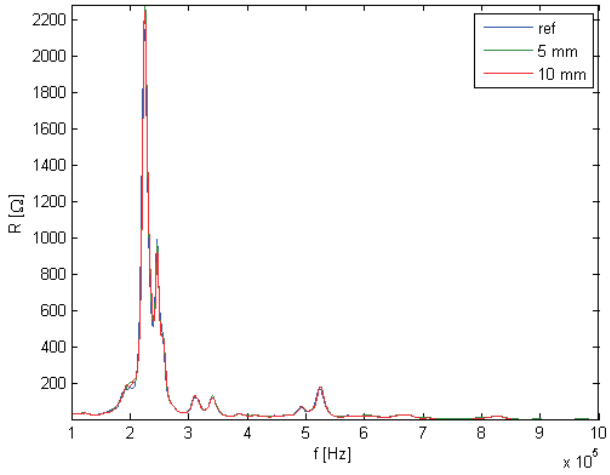

Figure 11: Resistance spectra for the three considered cases.

For damage detection purposes either conductance or resistance spectra can be investigated. In this research both were registered in large bandwidth up to 1 MHz. The resistance spectra is presented in Fig. 11 while the conductance spectra in Fig. 12. The curves were plotted from the frequency

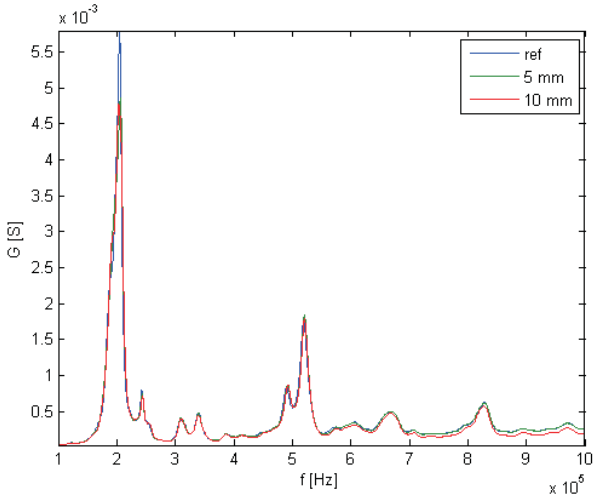

Figure 12: Conductance spectra for the three considered cases.

100 kHz. This is the basic frequency from which differences could be noticed. According to [1] it is advisable to consider in the EMI method the frequency band with most possible dynamic variability. Comparing the resistance (Fig. 11) and conductance spectra (Fig. 12) one can notice far more visible resonances in the case of conductance. For this reason this quantity was selected for further study. In order to assess the damage influence on the conductance spectra two indexes were used. The first one is a root mean square deviation, defined as

$$RMSD = 100\% \sqrt{\frac{\sum (x_i - x_{ref,i})^2}{\sum x_{ref,i}^2}}\,, \tag{2}$$

where x_i – denotes a conductance value of ith frequency for the damage case and $x_{ref,i}$ is the conductance value of ith frequency for the reference case. The second one is correlation coefficient defined as

$$\mathrm{CC} = \frac{\mathrm{cov}(\mathrm{x}_i, x_{ref})}{\sqrt{\mathrm{cov}(\mathrm{x}_{ref})\mathrm{cov}(\mathrm{x_i})}}\,, \tag{3}$$

where $\mathrm{cov}(\cdot,\cdot)$ denotes a covariance of two variables and $\mathrm{cov}(\cdot)$ – a variance of the variable. The indexes were calculated for the whole frequency band, means from 100 kHz to 1000 kHz. Both indexes indicate changes in relation

to the reference state. The obtained values for RMSD index are gathered in Tab. 1. The values for the two damage cases (5 and 10 mm) are close. The obtained values for CC index are gathered in Tab. 2. The values for the two damage cases differ with sign and absolute value. The 5 mm damage case is characterized by more than 2.5 half larger absolute value of CC while for the 10 mm damage case the CC value is more than ten times lower.

Table 1: RMSD values for the three investigated cases.

Damage scenario	RMSD (100–1000 kHz)
0 mm	0.00
5 mm	14.43
10 mm	13.21

Table 2: CC values for the three investigated cases.

Damage scenario	CC/CC_{ref} (100–1000 kHz)
0 mm	1.00
5 mm	–2.56
10 mm	0.08

Both RMSD and CC indexes compare whole spectra or its parts. However, it is worth to look closer at local changes of the spectrum (Fig. 12). The attention was focused on the three highest resonances. The highest one occurs at frequency

$$f_{r1} = 204.731 \pm 0.020 \text{ kHz} \ , \tag{4}$$

the second one at

$$f_{r2} = 519.440 \pm 0.051 \text{ kHz} \, , \tag{5}$$

and the third one at

$$f_{r3} = 490.367 \pm 0.049 \text{ kHz} \ . \tag{6}$$

The considered damage cases cause shifts of these frequencies. The values of these shifts were gathered in Tab. 3. At the f_{r1} the shift is positive for

Table 3: Frequency shifts due to damage at the selected resonance frequencies.

Damagescenario	Δf [kHz] at f_{r1}	Δf [kHz] at f_{r2}	Δf [kHz] at f_{r3}
0 mm	0	0	0
5 mm	1.438+/–0.041	1.508+/–0.103	1.768+/–0.099
10 mm	–1.164+/–0.041	1.456+/–0.103	2.260+/–0.099

smaller damage and negative for larger damage. In the remaining cases (f_{r1} and f_{r2}) the shift is positive.

The conducted measurements and their analysis lead to an observation of spectra changes due to presence of damage. In order to combine all the obtained data in one analysis the three parameters CC, RMSD i Δf were calculated. They were calculated in percent change in relation to reference. Then they have been presented in a 3D space for comparison. The considered frequency shift was the one calculated at f_{r1}. The results were presented in Fig. 13. The results are well separated in the space allowing for damage detection. That happens because damage cases are separated for the reference case. Moreover it is possible to recognize the damage severity because the two damage cases are separated from each other.

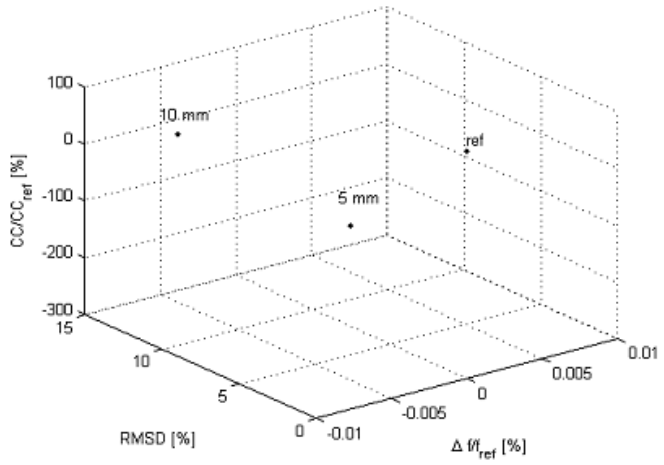

Figure 13: Damage detection results based on three parameter extracted from EMI measurements.

6 Conclusions

The results presented in this paper and related to guided wave propagation showed that considered phenomenon can be used for damage detection and localization in composite structural panels. Due to the orthotropic properties of laminated composites, guided wave velocities strictly depend on the direction of propagation. Moreover strong damping effect in composite materials should be taken into account. This effect is stronger for higher excitation frequencies. Excitation frequency should be appropriately chosen for given composite part by observing how far guided waves can propagate in the considered part.

Full-field measurements with combination of proposed signal processing algorithm allow to visualize internal structure of composite parts. This approach is very useful for parts with complex internal structure (stiffeners, honeycomb core, etc.) and complex geometry. This approach is also very sensitive for different types of simulated damage. However laser vibrometry connected with full-field measurements can be used only as a nondestructive testing method (NDT) or during development process of structural health monitoring system. In real SHM systems instead of laser vibrometry, network consisting of small number of piezoelectric transducer is used. In such a system only point-wise measurements are performed what give much smaller amount of signals and data for processing. It should be kept in mind that point-wise approach causes reduction of sensitivity to damage in relation to full-field measurement approach.

The research conducted regarding the EMI method showed the influence of damage presence on resistance and conductance spectra. The conductance has been used for further analysis because its spectrum was more higher in resonance peaks. Three parameters have been taken for the analysis and comparison of the reference case with two damage cases. The results are easily recognizable allowing for damage detection because damage cases are separated for the reference case. It was possible to recognize the damage severity because the two damage cases were separated from each other.

Acknowledgements Authors acknowledge partial support provided by projects IUVENTUS Plus No. IP2011 058971 and No. IP2011 033071 founded by the Ministry of Science and Higher Education. This research was also partially supported by the project entitled: Non–invasive Methods for Assessment of Physicochemical and Mechanical Degradation (PBS1/B6/8/2012) granted by National Centre for Research and Development in Poland.

Received 18 February, 2015

References

[1] Giurgiutiu V.: *Structural Health Monitoring with piezoelectric wafer active sensors*. Elsevier 2008.

[2] Raisutis R., Kazys R., Zukauskas E., Mazeika L., Vladisauskas A.: *Application of ultrasonic guided waves for non–destructive testing of defective CFRP rods with multiple delaminations*. NDT&E Int. **43**(2010), 416–424.

[3] Raisutis R., Kazys R., Zukauskas E. and Mazeika L.: *Ultrasonic air–coupled testing of square–shape CFRP composite rods by means of guided waves*. NDT&E Int. **44**(2011), 645–654.

[4] Mustapha S., Ye L., Wang D., Lu Y.: *Assessment of debonding in sandwich CF/EP composite beams using A0 Lamb wave at low frequency*. Compos. Struct. **93**(2011), 483–491.

[5] Kang T. Lee D.-H. Song S-J., Kim H.-J., Jo Y.-D., Cho H-J.: *Enhancement of detecting defects in pipes with focusing techniques*. NDT&E Int. **44**(2011), 178–187.

[6] Wang X., Tse P.W., Mechefske C.K., Hua M.: *Experimental investigation of reflection in guided wave-based inspection for the characterization of pipeline defects*. NDT&E Int. **43**(2010), 365–374.

[7] Rathod V.T., Mahapatra D.R.: *Ultrasonic Lamb wave based monitoring of corrosion type of damage in plate using a circular array of piezoelectric transducers*. NDT&E Int. **44**(2011), 628–636.

[8] Sohn H., Dutta D., Yang J.Y., Park H.J., De Simio M., Olson S., Swenson E.: *Delamination detection in composites through guided wave field image processing*. Compos. Sci. Technol. **71**(2011) 1250–1256.

[9] Chakraborty N., Rathod V.T., Mahapatra R.D., Gopalakrishnan S.: *Guided wave based detection of damage in honeycomb core sandwich structures*. NDT&E Int, **49**(2012), 27–33.

[10] Rhee I., Choi E., Roh S.-K.: *Guided wave propagation induced by piezoelectric actuator in bolted thin steel members KSCE*. J. Civil Eng. **16**(3), 2012, 398–406.

[11] Giurgiutiu V., Lin B., Santoni-Bottai G., Cuc A.: *Space application of piezoelectric wafer active sensors for structural health monitoring.* J. Intell. Mat. Syst. Str. **22**(80),2011, 1359–1370.

[12] Diamanti K., Soutis C. *Structural health monitoring techniques for aircraft composite structures.* Prog. Aerosp. Sci. **46**(2010), 342–352.

[13] Watkins R., Jha R. *A modified time reversal method for Lamb wave based diagnostics of composite structures.* Mech. Syst. Signal Pr. **31**(2012), 345–354.

[14] Giurgiutiu V., Soutis C.: *Enhanced composites integrity through structural health monitoring.* Appl. Compos. Mat. 2012, doi: 10.1007/s 10443–011–9247–2.

[15] Na J.K., Blackshire J.L. *Interaction of Rayleigh surface waves with a tightly closed fatigue crack.* NDT&E Int. **43**(2010) 432–439.

[16] t16 Chen X., Michaels J.E., Lee S.J., Michaels T.E.: *Load–differential imaging for detection and localization of fatigue cracks using Lamb waves.* NDT&E Int. **51**(2012), 142–149.

[17] Yeum C.M., Sohn H., Ihn J.B., Lim H.J.: *Instantaneous delamination detection in a composite plate using a dual piezoelectric transducer network.* Compos. Struct. **94**(2012), 3490–3499.

[18] Schubert K.J., Herrmann A.S.: *On the influence of moisture absorption on Lamb wave propagation and measurements in viscoelastic CFRP using surface applied piezoelectric sensors.* Compos. Struct. **94**(2012), 3635–3643.

[19] Yu L., Momeni S., Godinez V., Giurgiutiu V., Ziehl P., Yu J.: *Dual mode sensing with low-profile piezoelectric thin wafer sensors for steel bridge crack detection and diagnosis.* Adv. Civil Eng. **10**(2012), Hindawi doi:10.1155/2012/402179.

[20] Bhalla S., Gupta A., Bansal S. *et al.*: *Ultra low-cost adaptations of electro-mechanical impedance technique for structural health monitoring.* J. Intell. Mat. Syst. Str. **20**(2009), 991–999.

[21] Pohl J., Mook G.: *SHM of CFRP–structures with impedance spectroscopy and Lamb waves.* Int. J. Mech. Mat. Des. **6**(2010), 53–62.

[22] Park S., Park G., Yun C.-B. *et al.*: *Sensor Self–diagnosis using a modified impedance model for active sensing–based structural health monitoring.* Struct. Health Monit. – Int. J. **8**(2009), 71–82.

[23] Zagrai A.N., Giurgiutiu V.: *Electro-mechanical impedance method for crack detection in thin plates*. J. Intel. Mat. Syst. Str. **12**(2001), 709–718.

[24] Giurgiutiu V. and Kropas-Hughes C.: *Comparative study of neural-network damage detection from a statistical set of electro-mechanical impedance spectra*. Proc. SPIE 5047, 2002, doi: 10.1117/12.484050.

[25] Min J., Park S., Yun C.-B., Lee C.-G. and Lee C. *Impedance-based structural health monitoring incorporating neural network technique for identification of damage type and severity*. Eng. Struct. **39**(2012), 210–220.

[26] Filho J.V., Baptista F.G. and Inman D.J.: *Time-domain analysis of piezoelectric impedance–based structural health monitoring using multilevel wavelet decomposition*. Mech. Syst. Signal Pr. **25**(2011), 1550–1558.

[27] Park S., Inman D.J. and Yuna C.-B.: *An outlier analysis of MFC-based impedance sensing data for wireless structural health monitoring of railroad tracks*. Eng. Struct. **30**(2008), 2792–2799.

[28] Malinowski P., Wandowski T., Ostachowicz W.: *Characterisation of CFRP adhesive bonds by electromechanical impedance*. Proc. SPIE 9064, Health Monitoring of Structural and Biological Systems, 906415, 2014, doi: 10.1117/12.2042868.

[29] Park S., Kim J.-W., Lee C., Park S-K.: *Impedance–based wireless debonding condition monitoring of CFRP laminated concrete structures*. NDT&E Int. **44**(2011), 2011232–238.

[30] Palomino L.V., Steffen V.: *Damage metrics associated with electromechanical impedance technique for SHM applied to a riveted structure*. Proc. of 20th Int. Congress of Mechanical Engineering, Brazil, Gramado 2009.

[31] Ostachowicz W., Kudela P., Krawczuk M., Zak A., *Guided Waves in Structures for SHM: The Time – Domain Spectral Element Method*. Wiley 2012.

[32] An Y-K., Kim M.K., Sohn H.: *Airplane hot spot monitoring using integrated impedance and guided wave measurements*. Struct. Control Health Monitor. **19**(2012), 7, 592–604.

[33] Moharana S., Bhalla S.: *Influence of adhesive bond layer on power and energy transduction efficiency of piezo-impedance transducer*. J. Intell. Mat. Syst. Str., 2014, 1045389X14523858.

[34] Bhalla S., Moharana S.: *A refined shear lag model for adhesively bonded piezo-impedance transducers*. J. Intel. Mat. Syst. Str. **24**(2013), 1, 33–48.

[35] Wandowski T., Malinowski P., Ostachowicz W.: *Calibration problem of AD5933 device for electromechanical impedance measurements*. The e-J. Nondestruct. Test ISSN 1234-4934, **20**(2).

[36] Park S., Yun C-B., Roh Y. *et al.*: *Health monitoring of steel structures using impedance of thickness modes at PZT patches*. J. Smart Struct. Syst. **1**(2005), 4, 339–353.